ELSEVIER

Coastal Engineering 33 (1998) 137–154

COASTAL ENGINEERING

Observations of triad coupling of finite depth wind waves

I.R. Young [a,*], Y. Eldeberky [b,1]

[a] School of Civil Engineering, University College, Univ. of NSW, Canberra, ACT 2600, Australia
[b] Delft University of Technology, Delft, Netherlands

Received 23 October 1996; revised 15 December 1997; accepted 8 January 1998

Abstract

Fetch limited finite depth wind waves are subjected to a bispectral analysis to determine the extent of triad nonlinear coupling. Very long yet stationary time series are utilized, enabling the determination of bicoherence values with significantly smaller confidence limits than have been achieved previously. The bispectral analysis indicates a significant degree of phase coherence between the spectral peak frequency and higher frequencies. It is concluded that this phase coherence is as a result of non-resonant or bound triad interactions with the spectral peak frequency. Previous studies of triad coupling have generally been confined to relatively shallow water. Values of the relative depth, $k_p d$ (k_p is the wavenumber of the spectral peak, d is water depth) for these previous studies have ranged between 0.14 and 1.13. The present data set extends available data to values of $k_p d$ between 1.39 and 2.35. The existence of triad coupling at these water depths indicates that models which are to be used to predict waves in the transitional water depths found on many continental shelves may need to include the effects of such interactions. Previously, it has been assumed that triad interactions were generally only significant in the shoaling region. © 1998 Elsevier Science B.V.

Keywords: Finite depth wind waves; Non-resonant; Triad interactions; Phase coherence

* Corresponding author. E-mail: i-young@adfa.oz.au.
[1] Present address: International Research Centre for Computational, Hydrodynamics (ICCH), Danish Hydraulic Institute, Agern Allé 5, DK-2970 Hørsholm, Denmark. E-mail: yae@dhi.dk.

PII S0378-3839(98)00006-4

1. Introduction

The important role of quadruplet (four wave) interactions in the evolution of deep water wind wave spectra is well established (Hasselmann, 1962; Hasselmann et al., 1973; Young and Van Vledder, 1993). The progressive shift of energy to lower frequencies with fetch, the characteristic decay of the high frequency spectral tail and the unimodal spectral shape are all characteristics largely governed by quadruplet nonlinear interactions. In contrast, triad (three wave) interactions (Abreu et al., 1992) in deep water are insignificant (Phillips, 1960) in comparison to the quadruplet interactions.

In shallow water, however, the importance of triad interactions increases. Energy spectra of shoaling waves often show the appearance of harmonics of the spectral peak. Observations (Hasselmann et al., 1963; Elgar and Guza, 1985; Elgar et al., 1990, 1993) show that these harmonics are phase coherent with the spectral peak, indicating they are the result of triad interactions.

Due to the different nonlinear processes in these two regions, different modeling approaches have generally been adopted. In deep water, phase averaging or energy-based formulations (WAMDI group, 1988) have been applied. On the other hand phase resolving (e.g. Boussinesq) models have been utilized in shallow water (Peregrine, 1967, 1972, 1983; Freilich and Guza, 1984; Liu et al., 1985; Elgar et al., 1990) even extending into the surf zone (Schäffer et al., 1993; Eldeberky and Battjes, 1996).

Spectral models, such as WAM (WAMDI group, 1988) and SWAN (Booij et al., 1996), have also been applied to the intermediate water depths which occur on many continental shelves. The relative importance of triad interactions in such situations is, however, largely unknown. The vast majority of observations, suitable for determining triad nonlinear interactions have involved shoaling waves on beaches. Observations of the magnitude of triad interactions in wind generated waves in deeper, but finite depth, regions of the shelf are rare (Herbers and Guza, 1991). Hence, the applicability of models which ignore such processes is yet to be determined.

This paper presents the results of a bispectral analysis of fetch limited, intermediate depth wind waves. The data used for the analysis were taken from a shallow lake and hence are free from contamination by background swell. In addition, extremely long time series obtained under approximately constant wind conditions enable bispectral estimates with many degrees of freedom to be calculated.

The present data have been collected in deeper water than previous experiments which have considered bispectral analysis of waves. In addition, as the waves are propagating over an approximately horizontal bottom rather than a shelving beach, they will have a significantly broader directional spread than previous data.

The arrangement of the paper is as follows. Section 2 presents an overview of previous work on finite depth triad interactions and observations of the effects of such interactions. The experimental site and the conditions under which the present data set was collected are described in Section 3. The selection of data and the determination of bispectra are described in Section 4 with a detailed discussion of the observed bispectra in Section 5. Finally, the conclusions of the study are contained in Section 6.

2. Triad interactions

Nonlinear triad interactions can occur among waves with frequencies and wavenumbers which satisfy the relationships (Armstrong et al., 1962; Bretherton, 1964; Elgar et al., 1993)

$$f_1 \pm f_2 = f_3 \tag{1}$$

$$\boldsymbol{k}_1 \pm \boldsymbol{k}_2 = \boldsymbol{k}_3 \tag{2}$$

where f_i is the scalar frequency and $\boldsymbol{k}_i$ is the vector wavenumber, of the ith wave component. The components 1 and 2 each obey the linear dispersion relationship

$$\omega^2 = gk \tanh kd \tag{3}$$

where d is the water depth, $\omega = 2\pi f$ and $k = |\boldsymbol{k}|$ is the wavenumber magnitude.

Thus components which satisfy Eq. (1) and Eq. (2) can interact nonlinearly and exchange energy and momentum. Whilst the components 1 and 2 in Eq. (1) and Eq. (2) satisfy the dispersion relationship Eq. (3), component 3 may not necessarily satisfy Eq. (3). Interactions where component 3 satisfies the dispersion relationship $[\boldsymbol{k}_3 = \boldsymbol{k}(f_3)]$ are termed resonant interactions (Armstrong et al., 1962). Resonant interactions result in components at f_3 whose amplitudes can increase to be of the same order as the primary waves at f_1 and f_2. Note that for gravity surface waves this is only possible in very shallow water where the waves are nondispersive. Interactions where component 3 does not satisfy the dispersion relationship (Eq. (3)) are termed non-resonant (in intermediate water depths where waves are weakly dispersive—the so-called bound interaction of dispersive waves; Hasselmann, 1962). Non-resonant interactions result only in bound harmonics whose amplitudes remain small compared with those of the primary waves.

For spectra with a clearly defined major peak, one special case of the interaction conditions Eq. (1) and Eq. (2) which has been observed to be significant (for example, Hasselmann et al., 1963; Masuda and Kuo, 1981; Elgar and Guza, 1985; Doering and Bowen, 1987; Freilich et al., 1990; Elgar et al., 1990, 1993, 1995) is that where $f_1 = f_2 = f_p$, the frequency of the spectral peak. Such self interactions result in the generation of an harmonic of the spectral peak at $2f_p$. This form of interaction represents a convenient example to examine the implications of Eq. (1) and Eq. (2) on the form of the triad interaction. In shallow water, waves become non-dispersive and the dispersion relationship, Eq. (3) becomes $\omega = k\sqrt{gd}$. In such cases resonant interactions occur only for co-linear waves. In transitional water depths, where the waves are dispersive, only non-resonant or 'bound' triad interactions can occur.

Armstrong et al. (1962), Freilich and Guza (1984) and Elgar et al. (1993) have shown that significant energy transfers can also occur due to near-resonant interactions, in which the sum (or difference) component of the triad nearly satisfies the dispersion relationship. A measure of the departure from resonance can be obtained by defining $|\boldsymbol{k}_\delta|$ as the difference between the free wave component $|\boldsymbol{k}(f_3)|$, which satisfies the dispersion relationship, and the sum (or difference) ($|\boldsymbol{k}_1 \pm \boldsymbol{k}_2|$) wavenumber magnitudes

$$|\boldsymbol{k}_\delta| = |\boldsymbol{k}_1 \pm \boldsymbol{k}_2| - |\boldsymbol{k}(f_3)| \tag{4}$$

The wavenumber mis-match can be normalized as $\delta = |\boldsymbol{k}_\delta|/|\boldsymbol{k}(f_3)|$. The magnitude of δ determines the intensity of the energy exchange between the interacting waves. Zero mis-match represents the limiting case of the interaction process, in which the interacting waves remain intact and in phase (resonant interaction) during evolution. Thus, the magnitude of the energy transfer is maximum. When the mis-match is such that $\delta \ll 1$ (i.e. in the shoaling region), phase relations between the interacting waves vary slightly over a wavelength. Consequently the magnitudes and the sign of energy transfers between the interacting waves vary slowly over a wavelength, allowing significant net energy transfer over several wavelengths. Whereas resonant interactions are limited to nondispersive co-linear waves, near resonant interactions can occur between components separated by small angles (Elgar et al., 1993; Nwogu, 1994 and others).

The magnitude of triad interactions and the consequent energy transfer across the spectrum depend essentially on two factors. These are the order of magnitude of the nonlinearity determined by the relative wave amplitude, a/d and the shallowness of the water determined by the relative depth, $k_p d$, where a is the wave amplitude, d is the water depth and k_p is the wavenumber of the spectral peak. Increasing nonlinearity and decreasing relative depth intensifies the nonlinear rate of energy transfer across the spectrum.

Measurements to determine the magnitude of triad coupling in the wave field have concentrated on the determination of bispectra (Hasselmann et al., 1963; Lii et al., 1976; Kim and Powers, 1979, see S4). Hasselmann et al. (1963) considered the bispectra of waves measured in 11 m water depth. They found clear triad coupling with the spectral peak. The observed bispectra agreed well with the theoretical bispectra for a Stokes type expansion. Hence, it was concluded that non-resonant or bound triad interactions were responsible for the observed coupling.

Various studies have investigated shoaling waves with stations located at a number of water depths. Elgar and Guza (1985, 1986) investigated the bispectra of waves as they propagated from 9 m water depth to 1 m. Bicoherence values increased as the water depth decreased, indicating an increase in nonlinear coupling. In addition, as the water depth decreased the waves progressively became more ‘pitched forward’. Freilich et al. (1990) compared high resolution directional spectra measured at 10 m and 4 m. They found that linear shoaling theory was incapable of predicting the increase in energy observed at $2f_p$, which they attributed to near-resonant triad interactions. Elgar et al. (1993) also found significant near-resonant triad coupling for laboratory shoaling waves. Herbers et al. (1992) investigated near bottom wave orbital velocity and pressure measurements in a water depth of 7 m. Assuming that the waves had a relatively narrow directional spread due to the effects of refraction, they showed that forced waves at $2f_p$ were well modelled by the second order theory of Hasselmann (1962).

Abreu et al. (1992) abandoned the usual approach of modeling nonlinear shoaling waves in terms of the Boussinesq equations. Instead, they adopted the phase averaging energy based approach commonly used in deep water (WAMDI group, 1988). A source term for the energy balance equation was developed for the case of shallow water nondispersive co-linear triad interactions. The resulting model was compared with the data of Freilich et al. (1990). Model results were consistent with the data, leading Abreu et al. (1992) to conclude that the nonlinear coupling observed in these data was due to resonant co-linear interactions rather than near-resonant interactions, as concluded by Freilich et al. (1990).

Elgar et al. (1995) investigated both the bispectra and trispectra of wind sea spectra as they shoaled from 13 m water depth to 8 m water depth. They found significant triad coupling between the peak and $2f_p$. Analysis of the trispectra revealed that apparent triad coupling between the peak and $3f_p$ was misleading. The apparently significant bispectral levels were the result of tertiary or four wave interactions.

The experiments described above have almost exclusively dealt with the situation of shoaling waves on a beach. Beji and Battjes (1993) investigated waves propagating over a bar in the laboratory. They found strong phase coupling between spectral components at the peak, f_p and $2f_p$.

3. Experimental site and conditions

The data discussed here were collected in Lake George near Canberra, Australia. Lake George is approximately 20 km long by 10 km wide (Fig. 1). The lake bathymetry is very regular with a gradual bed slope from west to east and an average water depth of approximately 2 m. The data presented here were collected as part of a larger study to investigate fetch limited growth of finite depth wind waves (Young and Verhagen, 1996a,b; Young et al., 1996). Data were collected continuously at a rate of 8 Hz from a surface piercing Zwarts Pole (Zwarts, 1974) at the location shown in Fig. 1. Both easterly and westerly winds (perpendicular to the long shorelines) are common and careful scanning of the approximately 6 months of continuous data enabled the selection

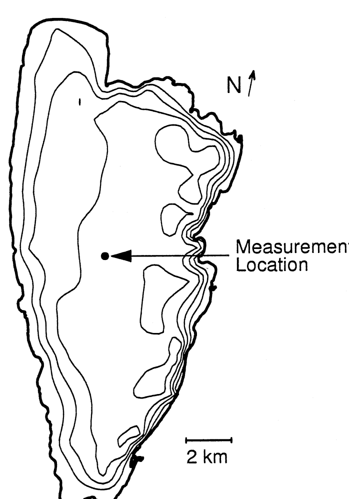

Fig. 1. Map of the measurement site at Lake George. The contour interval is 0.5 m with a maximum contour value of 2.0 m. Data were collected at the location shown during easterly and westerly conditions.

Table 1
Summary of the data collected

Quantity	Units							
Date	dd-mm-yy	25-10-93	29-10-93	6-11-93	4-12-93	7-12-93	15-12-93	8-1-94
U	m/s	11.5	8.0	5.0	11.0	6.7	9.5	13.2
σ_U	m/s	1.28	0.59	1.17	1.18	0.47	0.92	0.81
θ	°	274.4	278.1	276.1	263.4	100.5	281.1	271.4
σ_θ	°	12.3	7.6	6.5	5.8	9.9	6.4	6.8
T	h	7.26	6.39	8.71	6.97	7.96	9.95	10.92
ν	–	1634	1436	1960	1568	1792	2238	2456
H_s	m	0.42	0.30	0.19	0.38	0.26	0.34	0.44
f_p	Hz	0.41	0.47	0.53	0.43	0.50	0.46	0.40
$k_p d$	–	1.56	1.95	2.35	1.61	2.07	1.77	1.39
a/d	–	0.100	0.071	0.047	0.094	0.064	0.085	0.119
$b^2(f_p, f_p)$	–	0.071	0.038	0.014	0.060	0.035	0.049	0.166
A_s	–	−0.111	−0.105	−0.070	−0.096	−0.099	−0.095	−0.047
S_k	–	0.198	0.137	0.093	0.181	0.135	0.171	0.336

Quantities shown include: U—the mean wind speed measured at a reference height of 10 m; σ_U—the standard deviation of the wind speed; θ—the mean wind direction; σ_θ—the standard deviation of the wind direction; T—the length of the time series; ν—the number of degrees of freedom for the time series; H_s—the significant wave height; f_p—the frequency of the spectral peak; $k_p d$—the wavenumber of the spectral peak times the water depth; a/d—the relative depth, where $a = H_s/2$; $b^2(f_p, f_p)$—the bicoherence for self interactions involving the spectral peak; A_s—the asymmetry; S_k—the skewness.

of long time series with relatively constant wind speed and direction. Careful selection of the meteorological conditions, together with the absence of tidal water level variations, means that extremely long yet stationary time series can be obtained. Details of the data collected are summarized in Table 1.

The time series varied in duration from 6.39 h to 10.92 h. Typical examples of the variation of wind speed and direction during these extended time series are shown in Fig. 2. Although the time series were selected so as to have approximately constant wind speed and direction, whether the time series are truly stationary must be considered. The 10 min average values of both wind speed and direction were analyzed using the Run Test for Stationarity (Bendat and Piersol, 1971). The hypothesis that each of the time series was stationary was found to be accepted at the 10% level of significance.

Wind speeds range from 5.0 m/s to 13.2 m/s. The potential magnitude of finite depth effects can be determined from the quantity $k_p d$. Values range from 1.39 to 2.35. Values of $k_p d > \pi$ are generally considered to be deep water, whilst $k_p d < 0.25$ represent shallow water. Hence, the present data set is in transitional water depth. Most previous studies of triad coupling have concerned relatively long shoaling waves and are represented by values of $k_p d$ between 0.14 and 1.13. Hence, the present data set extends such investigations into deeper water. In addition, the present data set concerns fetch limited wind waves on an approximately horizontal bottom, rather than a mixture of swell and wind sea propagating over a sloping bathymetry. Refraction over such sloping bathymetry tends to narrow the directional spreading of the spectrum. Hence, the present data could be expected to have broader spreading than previously reported studies.

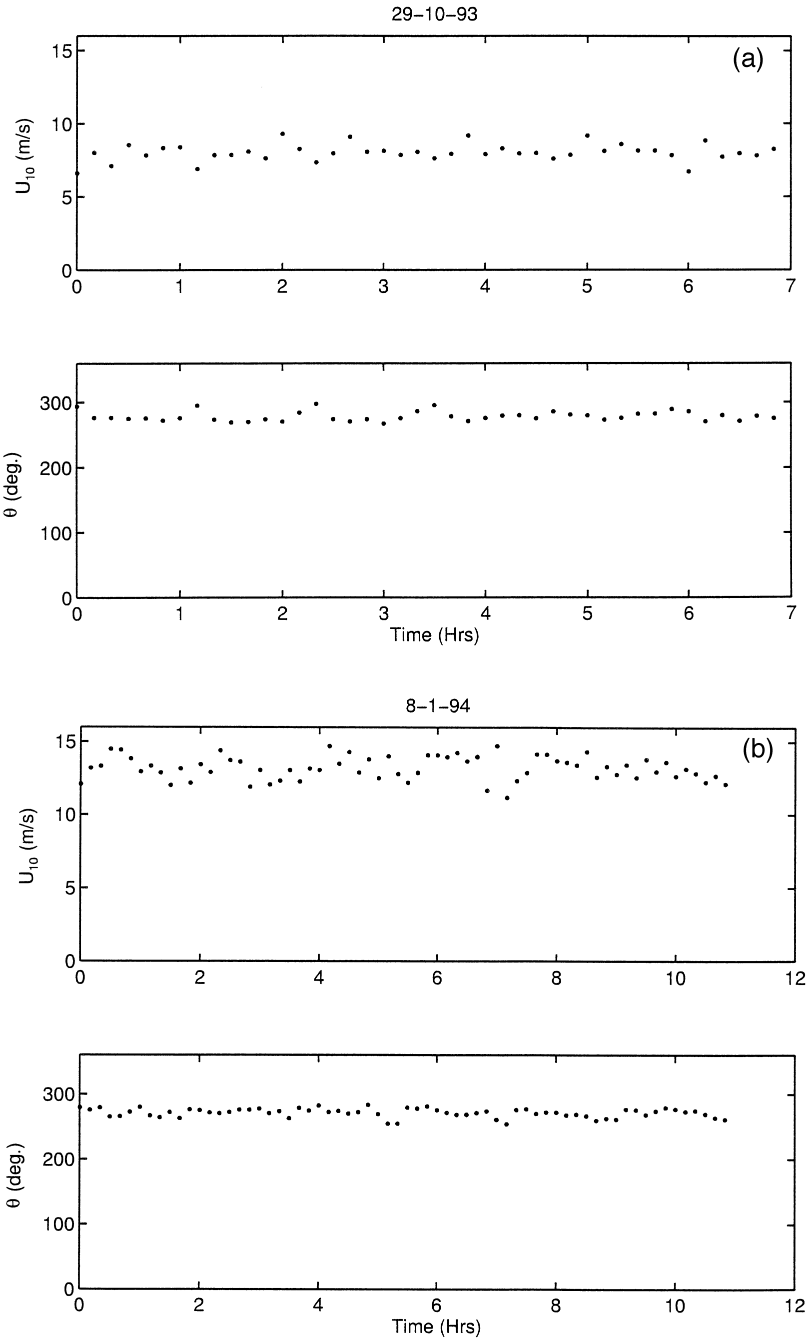

Fig. 2. (a) Values of wind speed (U_{10}) and direction (θ) as a function of time for the time series recorded on 29-10-93. Values shown represent averages over a period of 10 min. (b) Values of wind speed (U_{10}) and direction (θ) as a function of time for the time series recorded on 8-1-94. Values shown represent averages over a period of 10 min.

4. Data processing

4.1. Bispectral analysis

The bispectrum is formally defined as the Fourier transform of the third-order correlation function of the time series (Hasselmann et al., 1963). For a discretely sampled time series, this becomes

$$B(f_1,f_2)=E[X(f_1)X(f_2)X^*(f_1+f_2)] \tag{5}$$

where $E[]$ denotes the expected value or mean, $X(f)$ is the complex Fourier coefficient and the asterisk represents the complex conjugate.

The bispectrum can be recast into its normalized magnitude (Kim and Powers, 1979)

$$b_2(f_1,f_2)=\frac{|B(f_1,f_2)|^2}{E\left[|X(f_1)X(f_2)|^2\right]E\left[|X(f_1+f_2)|^2\right]} \tag{6}$$

where $b^2(f_1,f_2)$ is termed the bicoherence. The bicoherence is in the range $0 \le b^2 \le 1$, and is a measure of the phase coherence between spectral components at f_1, f_2 and $f_3=f_1+f_2$. A value of $b^2=1$ indicates complete coherence whilst $b^2=0$ indicates no coherence.

For a finite length time series statistical uncertainty will be introduced into the estimate of b^2. Hinich (1982) and Elgar and Sebert (1989) have shown that the bicoherence follows a noncentral χ^2 probability distribution which is a function of the number of degrees of freedom of the estimate of the Fourier transform and the true value of the bicoherence. The magnitude of the confidence limits increases as both the number of degrees of freedom and the true value of b^2 decrease. The dependence on the true value of b^2 complicates the estimation of confidence limits for bicoherence. Elgar and Sebert (1989) recommend the use of maximum likelihood estimates for the confidence limits to overcome this difficulty.

The probability distribution for bicoherence demonstrates the difficulty of obtaining statistically reliable estimates of this quantity when the bicoherence is low. Hence, if such estimates are to be attempted, very long (many degrees of freedom) time series are required.

The bicoherence determines whether there is phase coherence between spectral components. The details of the phase coherence can be obtained by examination of the relative magnitudes of the real and imaginary parts of the bispectrum. One representation is in terms of the biphase, $\beta(f_1,f_2)$

$$\beta(f_1,f_2)=\arctan\left\{\frac{\mathrm{Im}[B(f_1,f_2)]}{\mathrm{Re}[B(f_1,f_2)]}\right\} \tag{7}$$

Masuda and Kuo (1981) have shown that a spectral component and its harmonic with zero biphase is associated with the Stokes wave form with peaked crests and flat troughs. In contrast, as β approaches $-\pi/2$ the waves become increasingly pitched forward (a saw-tooth wave has $\beta = -\pi/2$). At low values of bicoherence care must be exercised as the biphase becomes unstable.

The nature of the phase coupling can also be determined using integrated properties of the bispectrum such as skewness, S_k and asymmetry, A_s.

$$S_k = \frac{\{\int\int \mathrm{Re}[B(f_1, f_2)] \mathrm{d}f_1 \mathrm{d}f_2\}}{[\overline{\eta^2}]^{3/2}} \quad (8)$$

$$A_s = \frac{\{\int\int \mathrm{Im}[B(f_1, f_2)] \mathrm{d}f_1 \mathrm{d}f_2\}}{[\overline{\eta^2}]^{3/2}} \quad (9)$$

where $\eta = \eta(t)$ is the water surface elevation and the overbar indicates the mean with respect to time. Positive values of skewness and negligible asymmetry correspond to Stokes type wave forms. Negative values of asymmetry indicate waves which are pitched forward.

4.2. Sampling considerations

The bicoherence values presented in Section 5 were obtained from time series sampled at 8 Hz. The time series were sub-divided into blocks of 256 points and the Fourier transform of each block determined. The Fourier coefficient product (5) was formed for each block and the products averaged to determine the bispectrum. The frequency resolution of the resulting bispectra was $\Delta f = 0.0313$ Hz. The time series used in this study are very long and hence there are a large number of degrees of freedom in the estimates of the Fourier coefficients. As shown in Table 1, the number of degrees of freedom vary between 1436 and 2456. Therefore, the resulting confidence limits are relatively small in magnitude (see Fig. 6) and weak triad coupling can be investigated.

5. Observed bispectra

The power spectra of the water surface elevation time series corresponding to the wind records shown in Fig. 2 appear in Fig. 3. In both cases the spectra are typical of fetch limited wind seas. They are unimodal with a high frequency face of the approximate form f^{-n}. In both cases, however, a slight 'hump' exists at $2f_p$. This feature is clear in these spectra due to the high number of degrees of freedom in the spectral estimates. In spectra obtained from 30 min time series (typical of most data gathering) such features are masked by the statistical variability of the spectral estimate.

The existence of the 'hump' at $2f_p$ is suggestive of the presence of triad self interactions involving the spectral peak. This is confirmed in Fig. 4 which shows

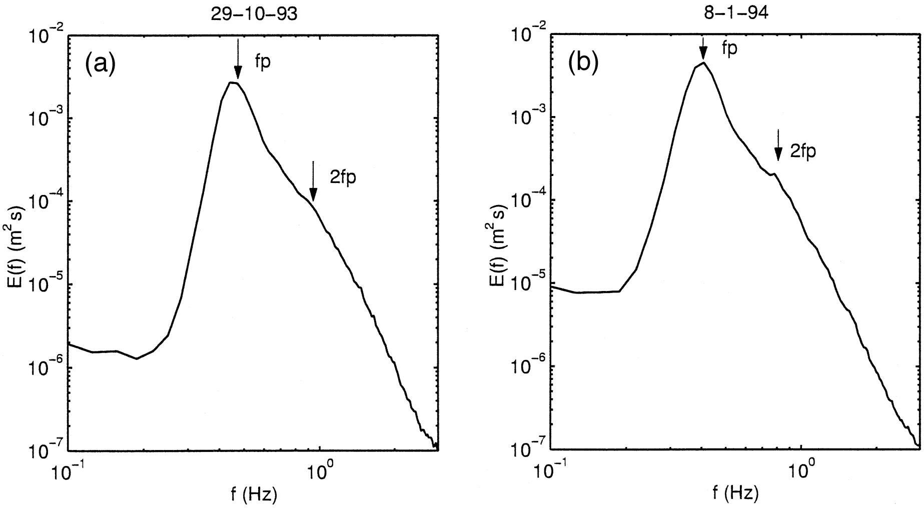

Fig. 3. (a) The power spectrum for the time series recorded on 29-10-93. The position of the spectral peak, f_p and twice the spectral peak, $2f_p$ are shown. (b) The power spectrum for the time series recorded on 8-1-94. The position of the spectral peak, f_p and twice the spectral peak, $2f_p$ are shown.

contour plots of the bicoherence, b^2 associated with these two cases. In both cases there is a peak at (f_p, f_p), indicating phase coherence between components with frequency f_p and $2f_p$. In addition, however, significant levels of bicoherence are present along the line $(f_1 \approx f_p,\ f_2)$. Thus it is concluded that, in addition to triad self coupling of the spectral peak, triad interactions between the peak and frequencies as high as $3f_p$ may also be present (Elgar et al., 1995). The contours shown in Fig. 4 are all above the 90% confidence limit for zero bicoherence.

Fig. 4a is for a wind speed of 8.0 m/s whilst Fig. 4b is for 13.2 m/s. Consequently, the relative wave amplitude, a/d is considerably larger and the relative depth $k_p d$ smaller in Fig. 4b than in Fig. 4a. The increased influence of the finite water depth (and also the finite amplitude) is clear in both the spectra of Fig. 3 ('hump' at $2f_p$ is larger for smaller $k_p d$) and the bispectra of Fig. 4 (b^2 larger for smaller $k_p d$). The phase coherence between components at the spectral peak and those at higher frequency increases as $k_p d$ decreases.

Values of bicoherence as a function of frequency are more clearly shown in Fig. 5 which shows $b^2(f_1 = f_p, f_2)$ as a function of frequency (i.e. a cut through the bicoherence parallel to one axis). A single dominant peak exists at $b^2(f_p, f_p)$ with values

Fig. 4. (a) Contours of the bicoherence, $b^2(f_1, f_2)$ for the time series recorded on 29-10-93. The contour interval is 0.01, with the minimum contour also 0.01. The frequency of the spectral peak is shown by the arrows. (b) Contours of the bicoherence, $b^2(f_1, f_2)$ for the time series recorded on 8-1-94. For clarity, an irregular contour interval has been used, with contours drawn at $b^2 = 0.01$, 0.02, 0.03, 0.04, 0.05, 0.10 and 0.15. The frequency of the spectral peak is shown by the arrows.

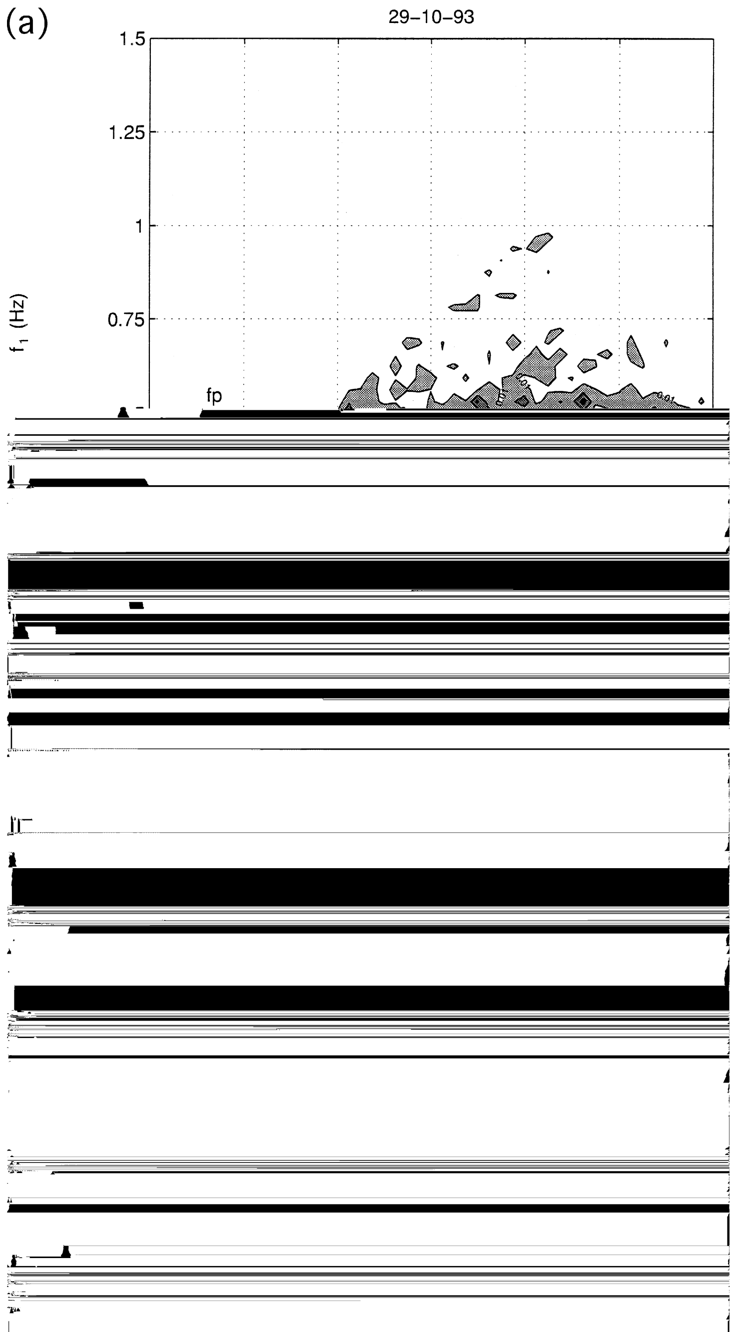
(a)
29–10–93
1.5
1.25
1
0.75
f1 (Hz)
fp

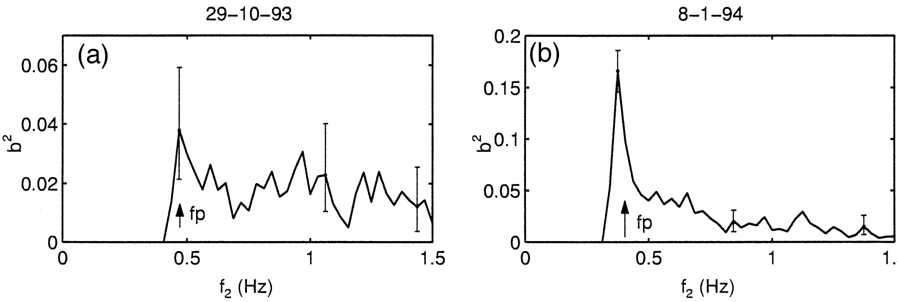

Fig. 5. (a) Values of $b^2(f_1 = f_p, f_2)$ (i.e. bicoherence values involving interactions with the spectral peak) as a function of frequency for the time series taken on 29-10-93. The position of the spectral peak is shown by the arrow. The error bars represent 95% confidence limits of the estimates of b_2. (b) Values of $b^2(f_1 = f_p, f_2)$ (i.e. bicoherence values involving interactions with the spectral peak) as a function of frequency for the time series taken on 8-1-94. The position of the spectral peak is shown by the arrow. The error bars represent 95% confidence limits of the estimates of b^2.

gradually decreasing at higher frequencies. As shown by the 95% confidence levels, however, these bicoherence values are still statistically significant. No bispectral peak appears at $(f_p, 2f_p)$ as is often observed for shoaling waves. This, however, is perhaps not surprising as no clear third harmonic $(3f_p)$ was present in the power spectra.

Values of $b^2(f_p, f_p)$ for all seven time series are shown as a function of the relative depth $k_p d$ in Fig. 6. The bicoherence clearly increases as the influence of finite depth increases. Even for the smallest value of $k_p d = 1.39$ these waves are still in transitional water depth and well above the non-dispersive shallow water limit. As these waves are still dispersive, the source of the phase coupling with the spectral peak appears to be

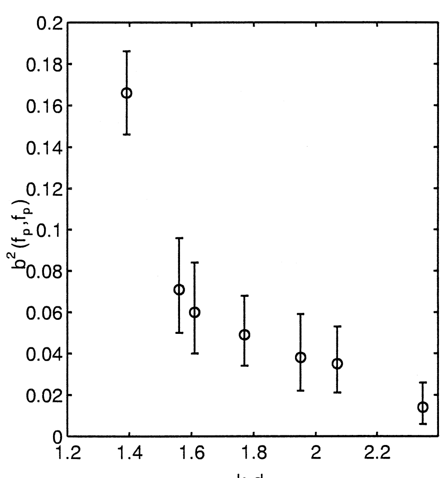

Fig. 6. Values of $b^2(f_p, f_p)$ (i.e. self interactions involving the spectral peak frequency) as a function of the relative depth $k_p d$. The error bars represent 95% confidence limits on the estimates of b^2.

non-resonant or bound triad interactions. Both resonant and near resonant interactions could not occur for such transitional depth dispersive waves.

It is interesting to compare the present observations with other published data sets. Elgar and Guza (1985) reported the evolution of shoaling waves at water depths from 9.0 m to 1.3 m. Values of $k_p d$ ranged from 0.14 to 0.37, significantly smaller than the values for the present data set. As the water depth decreased $b^2(f_p, f_p)$ increased from approximately 0.02 to 0.09. The spatial difference between the deepest and shallowest sites was approximately 300 m and the characteristic wavelength was of order 100 m. Hence, the triad interactions occurred over a distance of only a few wavelengths. Similarly, Freilich et al. (1990) observed values of $b^2(f_p, f_p)$ increasing from 0.04 to 0.36 as waves propagated shorewards from a depth of 10 m to a depth of 4 m. The transformation occurred over a distance of less than 5 wavelengths. Again, values of $k_p d$ were small, varying between 0.24 and 0.39. Based on bottom pressure records, Elgar et al. (1995) found significant coupling between the spectral peak and $2f_p$ for shoaling waves in deeper water (i.e. $k_p d = 0.67–1.13$).

The present data are obtained in even deeper water for which values of $k_p d$ vary between 1.39 and 2.35. Despite this, bicoherence levels are quite high, with $b^2(f_p, f_p) =$ 0.16 for the most depth dependent case. In contrast to shoaling data, however, the nonlinear interactions can occur over a very long distance. The downwind fetch is of order 1000 wavelengths compared to 5 for the shoaling data. Hence, although the magnitude of the triad coupling may be relatively weak, the extended distance over which it acts can result in measurable effects on the spectrum.

Herbers et al. (1992) considered shallower ($k_p d \approx 0.3–0.9$) but still intermediate depth (dispersive) waves and also found phase coupling between the spectral peak and $2f_p$. In addition, they found good agreement between their data and the second order theory of Hasselmann (1962). To make a comparison with the Hasselmann (1962) theory requires either high resolution directional data or an assumption that the spectrum has a narrow directional spread (e.g. shoaling waves on a beach). In the present case no directional data were available. In addition, the waves are fetch limited wind seas propagating over a horizontal bottom and have broad directional spreading (Young et al., 1996). Therefore, a comparison with the theory of Hasselmann (1962) is not feasible.

For a three wave system, Kim and Powers (1979) show that $b^2(f_1, f_2)$ represents the fraction of the energy at frequency $f_1 + f_2$ due to triad coupling of the three modes at f_1, f_2 and $f_1 + f_2$. For a broad band process a particular mode may simultaneously be involved in many interactions and such a simple interpretation of the bicoherence is not possible (McComas and Briscoe, 1980). However, Herbers and Guza (1992) argue that in such cases $b^2(f_1, f_2)$ can be interpreted as a lower bound on the energy at $f_1 + f_2$ which is nonlinearly coupled to f_1 and f_2. Hence, it can be concluded that, for the present data set, a substantial percentage ($> 10\%$) of the energy at $2f_p$ and above will be nonlinearly coupled to the spectral peak.

In the above discussion it has been assumed that the significant values of bicoherence observed are a result of triad coupling due to the finite water depth. Masuda and Kuo (1981) have, however, observed significant bispectral values for wind forced deep water waves. The wind forcing results in wave forms which are pitched forward (asymmetric).

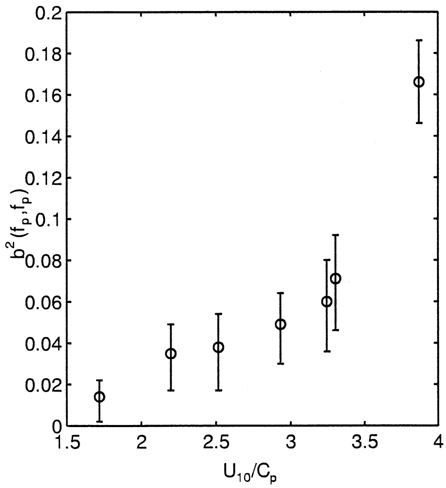

Fig. 7. Values of $b^2(f_p,f_p)$ (i.e. self interactions involving the spectral peak frequency) as a function of the inverse wave age U_{10}/C_p. The error bars represent 95% confidence limits on the estimates of b^2.

As the present data are both wind forced and finite depth, the relative contributions of the wind and the water depth must be considered. One means of assessing the importance of wind forcing to the observed nonlinear coupling is to plot $b^2(f_p,f_p)$ as a function of U_{10}/C_p, the inverse wave age (see Fig. 7), where C_p is the phase speed of components at the spectral peak. Fig. 7 shows $b^2(f_p,f_p)$ increasing with U_{10}/C_p, suggesting that increased nonlinear coupling is associated with increased wind forcing. This conclusion should, however, be treated with caution. The fetch and water depth are relatively constant for the present data set. Hence, decreasing values of $k_p d$ are always associated with increasing values of U_{10}/C_p as shown in Fig. 6 and Fig. 7. These forms of presentation cannot separate the relative contributions due to finite depth and wind.

An alternative is to investigate the relative magnitudes of the real and imaginary parts of the bispectrum as represented by the skewness and asymmetry. Fig. 8 shows S_k and A_s plotted as a function of the depth parameter, $k_p d$. As $k_p d$ decreases (or U_{10}/C_p increases), A_s remains relatively constant at approximately -0.1. There is no tendency for the waves to become progressively more pitched forward as the wind forcing increases. In contrast, S_k progressively increases as the relative water depth decreases. Therefore the waves become progressively more sharp crested as the influence of the finite depth increases. It can be concluded that, although wind forcing may lead to some of the observed nonlinear coupling for the present data set, non-resonant finite depth triad coupling is primarily responsible.

For $S_k < 0.2$, Ochi and Wang (1984) found virtually no deviation from the Gaussian probability density distribution for the sea surface elevation. Applying this criterion, the present data would suggest a limit of $k_p d \approx 1.5$, below which triad interactions become significant. Such a conclusion would, however, be misleading as $k_p d$ is not the sole parameter determining the significance of the triad interactions. The wave amplitude, a, is also an important parameter and, in the present case, the long propagation distance

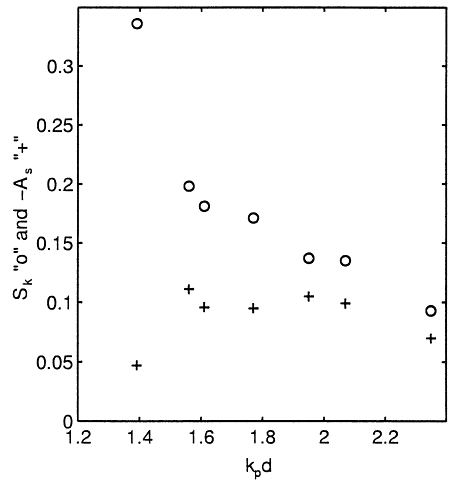

Fig. 8. Values of—asymmetry, A_k (crosses) and skewness, S_k (circles) as a function of the relative depth $k_p d$.

enables the energy transfer across the spectrum to assume measurable proportions. Hence, the propagation distance must also be assessed in determining the resultant influence on the evolution of the spectrum.

6. Conclusions

The results presented in this paper extend the parameter range of observations of triad interactions. Previous observations have largely been confined to shoaling waves. These have spanned both non-dispersion and dispersive cases, however, the maximum value of $k_p d$ has been limited to 1.13. In addition, since these observations have been confined to shoaling conditions, the effects of refraction have meant that the directional spreading in such cases has generally been narrow. In contrast, the present data set consists of fetch limited, dispersive intermediate depth water waves propagating over a horizontal bottom. Hence, the spectra will have broader directional spreading than in previous shoaling observations. The present data have also been collected in deeper water than previous observations (approximately twice as deep) with a maximum value of $k_p d =$ 2.35 for the present data set.

One might initially assume that the influence of triad interactions would be negligible for the present data set. A bispectral analysis of the data, however, clearly shows that a significant percentage ($> 10\%$) of energy at frequencies of $2 f_p$ and above is phase coherent with energy at the spectral peak. From this result, it is concluded that non-resonant or bound triad interactions can play a role in the evolution of fetch limited spectra in finite depth water.

The magnitude of the triad interactions for such transitional water depth waves will almost certainly be significantly smaller than those which occur for shoaling waves where significant spectral transformation can occur over a distance of a few wave-lengths.

Not surprisingly, the magnitude of the nonlinear coupling increased as the effects of depth limitation increased (as measured by the parameter $k_p d$). The spectra remained unimodal although the spectral tail would have been elevated by the nonlinear flow of energy away from the peak. The fact that a clear second harmonic ($2f_p$) was not present was possibly due to other processes such as quadruplet interactions which are known to have a shape stabilizing influence on the spectrum. The quadruplet interactions act to redistribute energy when a second, high frequency peak develops. The details of how bound energy at $2f_p$ and above would be influenced by quadruplet interactions is yet to be investigated in detail. Investigations of the effects of quadruplet interactions have largely been confined to free waves (Elgar et al., 1995).

In the discussion above, the concept of energy transfer has been introduced for non-resonant triad interactions. This is true in the sense that spectral components at the second harmonic ($2f_p$) have increased in magnitude. The whole concept of linear spectral analysis becomes questionable when nonlinear processes are introduced. Another way of considering the process is that the originally linear sinusoidal wave form has simply changed shape into a nonlinear (Stokes) form. There is still only one wave present, however it is no longer sinusoidal in form. Nevertheless, if spectral models such as SWAN (Booij et al., 1996) are to be used to model such intermediate water depth processes, the growth of the second harmonic can only be interpreted as an energy transfer.

However one wishes to interpret the process of non-resonant triad interaction, the consequences are important. An interesting example is the Beji–Battjes bar (Beji and Battjes, 1993). Deep water linear waves were incident on a shoal. As the waves propagated across the shoal, the magnitude of the second harmonic increased and the waves were clearly observed to take a nonlinear shape. The waves were still dispersive and hence non-resonant and near-resonant interactions were responsible for the growth of the harmonic. Holthuijsen (private communication) indicates that once these waves entered deep water again, the bound components at $2f_p$ were ‘set free’ to propagate at their respective linear group velocities. Although the appearance of the second harmonic over the shoal may be considered as a spurious artefact resulting from the linear spectral representation of a nonlinear wave, these components became real once they entered deep water. The conclusion is clear; if the linear spectral representation is to be retained in intermediate water depth, non-resonant interactions can be interpreted as an energy transfer to the bound harmonic components.

The significance of this study is that it raises the possibility that triad interactions may play a role in the evolution of waves in transitional water depth such as is found on most continental shelves. As such, it may be necessary to include such processes in wave models used to predict waves in intermediate water depth. To date, it has been assumed that such processes need only be included in the shoaling region.

Acknowledgements

The data collection process would have been impossible without the considerable assistance of Louis Verhagen and Astrid Van Agthoven, their efforts are appreciated.

The project was funded by the Australian Research Council, without which it would have been impossible. This contribution is gratefully acknowledged.

References

Abreu, M., Larraza, A., Thornton, E., 1992. Nonlinear transformation of directional wave spectra in shallow water. J. Geophys. Res. 97, 15579–15589.

Armstrong, J.A., Bloembergen, N., Ducuing, J., Pershan, P.S., 1962. Interactions between light waves in a nonlinear dielectric. Phys. Rev. 127, 1918–1939.

Beji, S., Battjes, J.A., 1993. Experimental investigation of wave propagation over a bar. Coastal Eng. 19, 151–162.

Bendat, J.S., Piersol, A.G., 1971. Random Data: Analysis and Measurement Procedures. Wiley-Interscience, New York, p. 407.

Booij, N., Holthuijsen, L.H., Ris, R.C., 1996. The SWAN wave model for shallow water. Int. Conf. Coastal Eng., Orlando.

Bretherton, F.P., 1964. Resonant interactions between waves: The case of discrete oscillations. J. Fluid Mech. 20, 457–480.

Doering, J.C., Bowen, A.J., 1987. Skewness in the nearshore zone: A comparison of estimates from Marsh–McBirney current meters and colocated pressure sensors. J. Geophys. Res. 92, 13173–13183.

Eldeberky, Y., Battjes, J.A., 1996. Spectral modeling of wave breaking: application to Boussinesq equations. J. Geophys. Res. 101, 1253–1264.

Elgar, S., Guza, R.T., 1985. Observations of bispectra of shoaling surface gravity waves. J. Fluid Mech. 161, 425–448.

Elgar, S., Guza, R.T., 1986. Nonlinear model predictions of bispectra of shoaling surface gravity waves. J. Fluid Mech. 167, 1–18.

Elgar, S., Sebert, G., 1989. Statistics of bicoherence and biphase. J. Geophys. Res. 94, 10993–10998.

Elgar, S., Freilich, M., Guza, R.T., 1990. Model–data comparisons of moments of nonbreaking shoaling surface gravity waves. J. Geophys. Res. 95, 16055–16063.

Elgar, S., Guza, R.T., Freilich, M.H., 1993. Observations of nonlinear interactions in directionally spread shoaling surface gravity waves. J. Geophys. Res. 98, 20299–20305.

Elgar, S., Herbers, T.H.C., Chandran, V., Guza, R.T., 1995. Higher-order spectral analysis of nonlinear ocean surface gravity waves. J. Geophys. Res. 100, 4983–4997.

Freilich, M.H., Guza, R.T., 1984. Nonlinear effects on shoaling surface gravity waves. Philos. Trans. R. Soc. London, Ser. A 311, 1–41.

Freilich, M.H., Guza, R.T., Elgar, S., 1990. Observations of nonlinear effects in directional spectra of shoaling surface gravity waves. J. Geophys. Res. 95, 9645–9656.

Hasselmann, K., 1962. On the non-linear energy transfer in a gravity-wave spectrum: 1. General theory. J. Fluid Mech. 12, 481–500.

Hasselmann, K., Munk, W., MacDonald, G., 1963. In: Rosenblatt, M. (Ed.), Bispectra of Ocean Waves. Time Series Analysis. Wiley, New York, pp. 125–139.

Hasselmann, K. et al., 1973. Measurements of wind-wave growth and swell decay during the Joint North Sea Wave Project (JONSWAP). Dtsch. Hydrographische Z. 8, 12, Suppl. A.

Herbers, T.H.C., Guza, R.T., 1991. Wind-wave nonlinearity observed at the sea floor: Part I. Forced-wave energy. J. Phys. Oceanogr. 21, 1740–1761.

Herbers, T.H.C., Guza, R.T., 1992. Wind-wave nonlinearity observed at the sea floor: Part II. Wavenumbers and third-order statistics. J. Phys. Oceanogr. 22, 489–504.

Herbers, T.H.C., Lowe, R.L., Guza, R.T., 1992. Field observations of orbital velocities and pressure in weakly nonlinear surface gravity waves. J. Fluid Mech. 245, 413–435.

Hinich, M.J., 1982. Testing for Gaussianity and linearity of a stationary time series. J. Time Ser. Anal. 3, 66–74.

Kim, Y.C., Powers, E.J., 1979. Digital bispectral analysis and its application to nonlinear wave interactions. IEEE Trans. Plasma Sci., pp. 120–131.

Lii, K.S., Rosenblatt, M., Van Atta, C., 1976. Bispectral measurements in turbulence. J. Fluid Mech. 77, 45–62.

Liu, P.L.-F., Yoon, S.B., Kirby, J.T., 1985. Nonlinear refraction–diffraction of waves in shallow water. J. Fluid Mech. 153, 185–201.

Masuda, A., Kuo, Y., 1981. A note on the imaginary part of bispectra. Deep Sea Res., Part A 28, 213–222.

McComas, C.H., Briscoe, M.G., 1980. Bispectra of internal waves. J. Fluid Mech. 97, 205–213.

Nwogu, O., 1994. Nonlinear evolution of directional wave spectra in shallow water. Proc. 24th Conf. on Coastal Eng., Vol. 1, Kobe, pp. 467–481.

Ochi, M.K., Wang, W.C., 1984. Non-Gaussian characteristics of coastal waves. Proc. 19th Int. Conf. on Coastal Eng., Vol. 1, Houston, pp. 516–531.

Peregrine, D.H., 1967. Long waves on a beach. J. Fluid Mech. 27, 815–827.

Peregrine, D.H., 1972. Equations for water waves and the approximations behind them. In: Meyer, R.E. (Ed.), Waves on Beaches and Resulting Sediment Transport. Academic Press, San Diego, CA, pp. 95–122.

Peregrine, D.H., 1983. Breaking waves on beaches. Annu. Rev. Fluid Mech. 15, 149–178.

Phillips, O.M., 1960. On the dynamics of unsteady gravity waves of finite amplitude: Part 1. The elementary interactions. J. Fluid Mech. 9, 193–217.

Schäffer, H.A., Deigaard, R., Madsen, P.A., 1993. A Boussinesq model for waves breaking in shallow water. Coastal Eng. 20, 185–202.

WAMDI group, 1988. The WAM model—A third generation ocean wave prediction model. J. Phys. Oceanogr. 18, 1775–1810.

Young, I.R., Van Vledder, G.Ph., 1993. The central role of nonlinear interactions in wind-wave evolution. Philos. Trans. R. Soc. London, Ser. A 342, 505–524.

Young, I.R., Verhagen, L.A., 1996a. The growth of fetch limited waves in water of finite depth: Part I. Total energy and peak frequency. Coastal Eng. 28, 47–78.

Young, I.R., Verhagen, L.A., 1996b. The growth of fetch limited waves in water of finite depth: Part II. Spectral evolution. Coastal Eng. 28, 79–100.

Young, I.R., Verhagen, L.A., Khatri, S.K., 1996. The growth of fetch limited waves in water of finite depth: Part III. Directional spectra. Coastal Eng. 28, 101–122.

Zwarts, C.M.G., 1974. Transmission line wave height transducer. Int. Symp. on Wave Measurement and Analysis, pp. 605–620.